Clays and Clay Minerals, Vol. 42, No. 3, 288–297, 1994.

EFFECTS OF THE STRUCTURE OF SILICA-ALUMINA GEL ON THE HYDROTHERMAL SYNTHESIS OF KAOLINITE

SHIGEO SATOKAWA,[1]* YASUSHI OSAKI,[2] SOICHIRO SAMEJIMA,[2] RITSURO MIYAWAKI,[3] SHINJI TOMURA,[3] YASUO SHIBASAKI,[3] AND YOSHIYUKI SUGAHARA[4]

[1] Engineering Research Association for Artificial Clay, National Industrial Research Institute of Nagoya, Kita, Nagoya 462, Japan

[2] Chemical Research Laboratory, Tosoh Corporation, Shin-nanyo, Yamaguchi 746, Japan

[3] Ceramic Technology Department, National Industrial Research Institute of Nagoya, Kita, Nagoya 462, Japan

[4] Department of Applied Chemistry, Waseda University, Ohkubo, Shinjuku, Tokyo 169, Japan

Abstract—Kaolinite was hydrothermally synthesized from two kinds of silica-alumina gels to examine the effect of the structure of the starting material. Two kinds of gels were prepared by precipitation at different pH conditions (pH = 9.6 and 4.2) from solutions containing water glass and aluminum sulfate. Na ions in the gels were removed with a resin before the hydrothermal treatment, but a slight amount of sulfate ions was still present in the gels. The nuclear magnetic resonance spectra of the starting gels suggested that the gel prepared at pH 9.6 consists of networks with alternating SiO_4- and AlO_4-tetrahedra (partially AlO_6-octahedra), whereas the gel prepared at pH 4.2 consists of a sheet structure related to allophane. After the hydrothermal treatment at 220°C for 9 days, kaolinite particles with spherical shape were obtained from the former gel, and platy kaolinite was crystallized from the latter one. The difference in morphology of synthetic kaolinite was attributable to the structures of the starting gels, and the pH values in the hydrothermal reactions were not very significant to the morphology.

Key Words—Gel structure, Hydrothermal synthesis, Kaolinite, Nuclear magnetic resonance, Silica-alumina gel.

INTRODUCTION

A number of minerals, reagents, and gels have been examined as a starting material for the synthesis of kaolinite. The first study on the synthesis of kaolinite from silica-alumina gel was reported by Ewell and Insley (1935). Roy and Osborn (1954) revealed the outline of the phase equilibrium between kaolinite and related phases, based on their systematic study of the Al_2O_3–SiO_2–H_2O system. De Kimpe *et al.* (1961) examined the syntheses of aluminosilicates at low temperatures and under normal pressure with the gels and crystalline phases of various Si/Al proportions. They reported that kaolinite could be obtained at low pH, where the six-coordinated structure of Al is stabilized. Moreover, De Kimpe *et al.* (1964) found that the conditions of temperature, pH, and cationic or anionic impurities are critical for the formation of kaolin minerals.

Although various forms of synthetic kaolinites have been reported, only few papers have focused on the relationship between synthesis conditions and the mineralogical properties of the synthesized kaolinite. De Kimpe *et al.* (1964) reported that kaolin minerals with three forms (platy, lath-like, and rod-like) could be synthesized under different synthesis conditions. Tomura *et al.* (1983) reported the synthesis of spherical kaolinite and its mineralogical properties. Tomura *et al.* (1985) also reported that the spherical kaolinite was mainly produced at higher solid to water ratio (1/4) and at lower temperatures (150°–200° C) than the conditions for the synthesis of platy kaolinite. Miyawaki *et al.* (1991) revealed that the addition of Li salt into the reaction system of the synthesis improved the crystallization of kaolinite along the (001) direction.

On the other hand, Léonard *et al.* (1964) and Fripiat *et al.* (1965) reported structural formulas and properties of amorphous aluminosilicates with various Al/Si ratios, and Cloos *et al.* (1969) proposed their schematic structural models. However, the effect of the structure of the starting material on the synthetic kaolinite was not clarified. Therefore, the authors investigated the hydrothermal process of kaolinite from silica-alumina gels having different local structures with magic angle spinning nuclear magnetic resonance (MAS/NMR), X-ray diffraction (XRD), and transmission electron microscopy (TEM).

* Present address: Fundamental Technology Research Laboratory, Tokyo Gas Co., Ltd., Shibaura, Minato, Tokyo 105, Japan.

EXPERIMENTAL METHODS

Materials

Silica-alumina gels were prepared from commercially available raw materials; water glass (Daiso Co., 99.9% purity; SiO_2 = 29.6 wt. %, Na_2O = 9.35 wt. %, Al_2O_3 = 0.01 wt. %) and Al sulfate aqueous solution (Kurosaki Chemical Industry Co., 99.5% purity; Al_2O_3 = 8.02 wt. %). Na silicate aqueous solution (1.0 M Na_2SiO_3) was prepared from a mixture of the water glass and a NaOH aqueous solution (Tosoh Co., 99.9% purity; NaOH = 48 wt. %), and the pH of the system was controlled by the amount of NaOH. The concentration of the Al sulfate aqueous solution was adjusted to 0.5 M. Both solutions were fed dropwise constantly (100 ml/min) at the same time and stirred in a reaction vessel at 40°C. The Si/Al molar ratio of the mixture was adjusted to 1.0, which was equal to that of kaolinite. Two kinds of gels were prepared under two different pH conditions (pH = 9.6 and 4.2; hereafter described as "gel-A" and "gel-B," respectively). These two pH values were selected from the solubility diagram of amorphous silica and $Al(OH)_3$ at 25°C (Pourbaix, 1991) (Figure 1). An Al ion is present as a four-coordinated ion in a basic solution with pH > 9, whereas it is present as a six-coordinated ion in an acidic solution of pH < 4. On the other hand, the solubility of $Al(OH)_3$ is low in the neutral pH range (pH = 4–9). Also, the solubilities of amorphous silica and $Al(OH)_3$ are almost equivalent at about pH = 4 and 9.

The removal of impurities (Na ions and sulfate ions) from the gels was carried out with the following procedure. The Na ions in gels-A and -B were removed with a strong cation exchange resin (Amberlite 200C). The gels were boiled for the removal of sulfate ions. After the removal of impurities, the gels were dried at 100°C for 24 h, and sieved to pass a #70 mesh (hereafter described as "gel-HA" and "gel-HB").

The hydrothermal treatment was carried out with 2 g of the gel and 18 ml of distilled water in a 25 ml Teflon pressure vessel (San-ai Kagaku Ltd., HU-25). The pressure vessel was kept at 220°C for 1, 3, 5, 7, or 9 days in a convectional dryer. The pH of the slurry was measured with a pH meter (Horiba, M8 AD) before and after the hydrothermal treatment. The solid products were separated by filtration, washed with distilled water, and dried at 100°C for 1 day.

The hydrothermal treatment was also carried out using gel-HA under an acidic condition with additional sulfuric acid. The initial pH of the slurry was adjusted to pH = 2, and the hydrothermal treatment was carried out at 220°C for 9 days in the pressure vessel.

Analytical methods

The gels and hydrothermal products were characterized by XRD, infrared spectroscopy (IR), ^{27}Al- and ^{29}Si-MAS/NMR, and differential thermal-thermogravimetric analysis (DTA-TG). The chemical compositions of the starting materials and hydrothermal products were analyzed by atomic absorption analysis for Na, Al, and Si using the samples that were decomposed by hydrofluoric acid and by X-ray fluorescence analysis for S. XRD patterns were obtained with graphite monochromatized Cu$K\alpha$ radiation (Rigaku RAD-IIB: 40 kV, 20 mA). IR spectra were recorded on a Jasco IR-700 spectrophotometer using the KBr method. ^{27}Al- and ^{29}Si-MAS/NMR spectra were obtained by a JEOL-GSX400 spectrometer (9.4 T) with 4 kHz spinning rate. The frequency of ^{27}Al-MAS/NMR spectra was 104.05 MHz, repetition time was 5 s, pulse width was 4.0–4.3 μs, and 200 free induction decays were accumulated. Chemical shifts were reported relative to external $Al(H_2O)_6^{3+}$. The frequency of ^{29}Si-MAS/NMR spectra was 79.30 MHz and the spectra were measured by two methods with and without cross polarization (CP). Repetition times were 5 s and 60 s, pulse width were 5.8 and 4.3 μs, and 2000 and 800 free induction decays were accumulated for the methods, respectively. Chemical shifts were reported relative to external tetramethylsilane (TMS). The DTA-TG analysis was carried out with 40 mg of each sample by heating from room temperature to 1150°C at a rate of 10°C/min, using a Rigaku TG8110-TAS100 thermal analyzer. The morphology of the products was observed by a transmission electron microscope (TEM) (JEOL, JEM-2000FX) operated at 100 kV. Specific surface area was measured for the samples by N_2 gas adsorption (the B.E.T. method) using a Carlo Erba Instruments, Sorptomatic 1800 analyzer. The samples were pretreated at 100°C under vacuum condition.

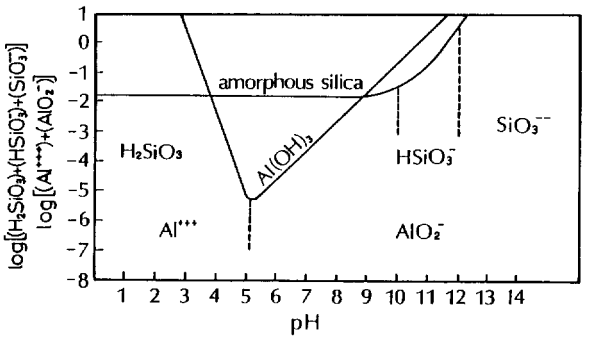

Figure 1. The solubility diagram of amorphous silica and aluminum hydroxide (gibbsite) at 25°C (after Pourbaix, 1991).

RESULTS

Gels

The XRD patterns showed that all the gels (gels-A, -B, -HA, and -HB) were amorphous. The chemical analysis of gels-A, -B, -HA, and -HB (Table 1) indicated that most of Na ions could be removed by the ion-

https://doi.org/10.1346/CCMN.1994.0420307 Published online by Cambridge University Press

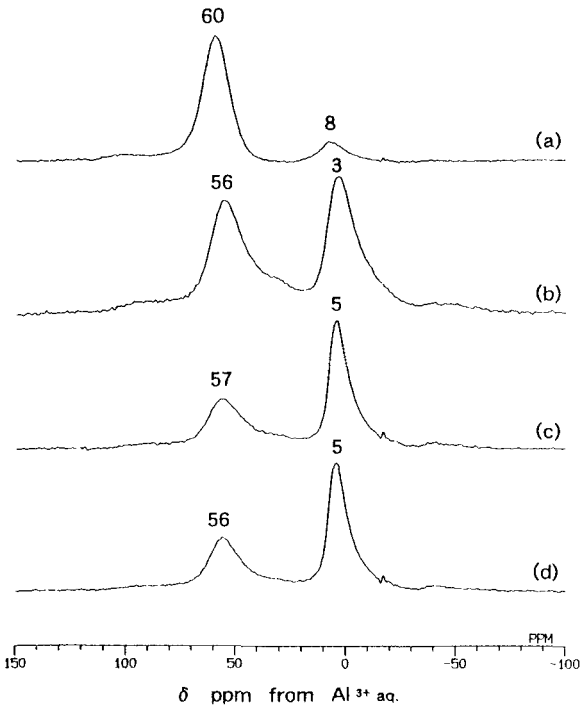

Figure 2. ^{27}Al-MAS/NMR spectra of a) gel-A, b) gel-HA, c) gel-B, and d) gel-HB.

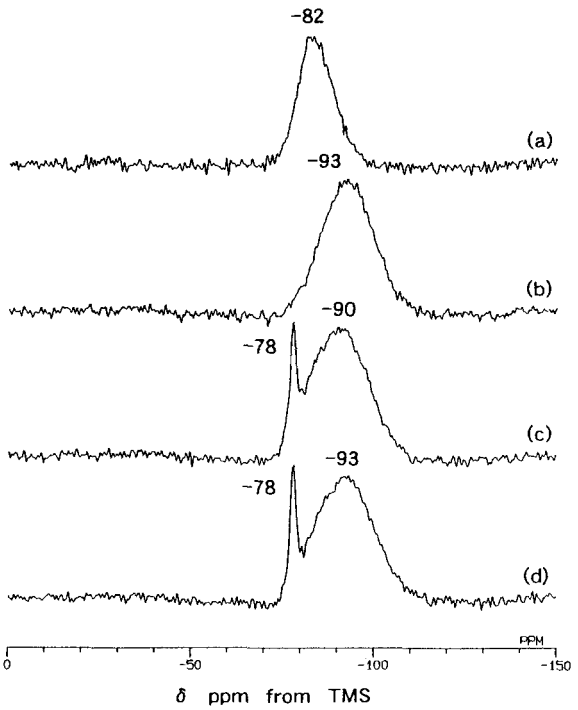

Figure 3. ^{29}Si-CP/MAS/NMR spectra of a) gel-A, b) gel-HA, c) gel-B, and d) gel-HB.

exchange treatment. However, the sulfate ions in gel-B could not be removed completely by boiling. The Al contents in gels-HA and -HB, which were obtained by the removal of impurities, were less than those in the original gels (gels-A and -B). The Si/Al ratios of the ion-exchanged gels-HA and -HB were slightly higher, 1.06 and 1.18, compared with the ideal one for kaolinite, 1.00. The water content in the gel was estimated from the weight loss between room temperature and 1000°C recorded on the TG curve. The water content in gel-HA (27.4%) was greater than that in gel-A (17.5%).

The ^{27}Al-MAS/NMR spectra of gels-A, -B, -HA, and -HB showed two peaks at about 5 and 60 ppm, but the relative intensities of the two resonances in each spectrum were different (Figure 2). Gel-A showed the resonance corresponding to four-coordinated Al atoms at 60 ppm as a major peak, in contrast to gel-B whose dominant resonance corresponded to six-coordinated Al atoms at 5 ppm. The relative intensity of the peak at 8 ppm corresponding to six-coordinated Al atoms of gel-A was increased after the removal of impurities (gel-HA), whereas the spectrum of gel-HB was similar to that of gel-B.

Table 1. Atomic ratios of gels.

Sample	Na/Al	S/Al	Si/Al
Gel-A	0.72	n.d.[1]	0.94
Gel-B	0.10	0.02	0.96
Gel-HA	0.02	n.d.[1]	1.06
Gel-HB	0.01	0.03	1.18

[1] Not detected.

The ^{29}Si-MAS/NMR spectra of gels-A, -B, -HA, and -HB were measured with CP technique (Figure 3). The features of these spectra were very similar to those obtained without the CP technique. The ^{29}Si spectra of gels-A and -HA showed broad resonances at −82 and −93 ppm, respectively, and the spectra of gels-B and -HB showed a sharp peak at −78 ppm, superimposed on a broader feature centered at −90 and −93 ppm, respectively.

Transmission electron micrographs of gels-HA and -HB are shown in Figures 4a and 4d. Both gels showed the typical appearance of amorphous materials.

Hydrothermal products

The XRD patterns of gel-HA and its hydrothermal products are shown in Figure 5a. The 001 and 002 reflections of kaolinite were observed at 7.1 and 3.6 Å for the product obtained after 1 day. The intensity of the diffraction peaks gradually increased with reaction time. The intensities of the kaolinite-peaks of the products obtained by the reaction for 5, 7, and 9 days were almost equivalent, suggesting a saturation of the crystallization within 5 days. The product obtained by the synthesis for 9 days (hereafter described as "product-

https://doi.org/10.1346/CCMN.1994.0420307 Published online by Cambridge University Press

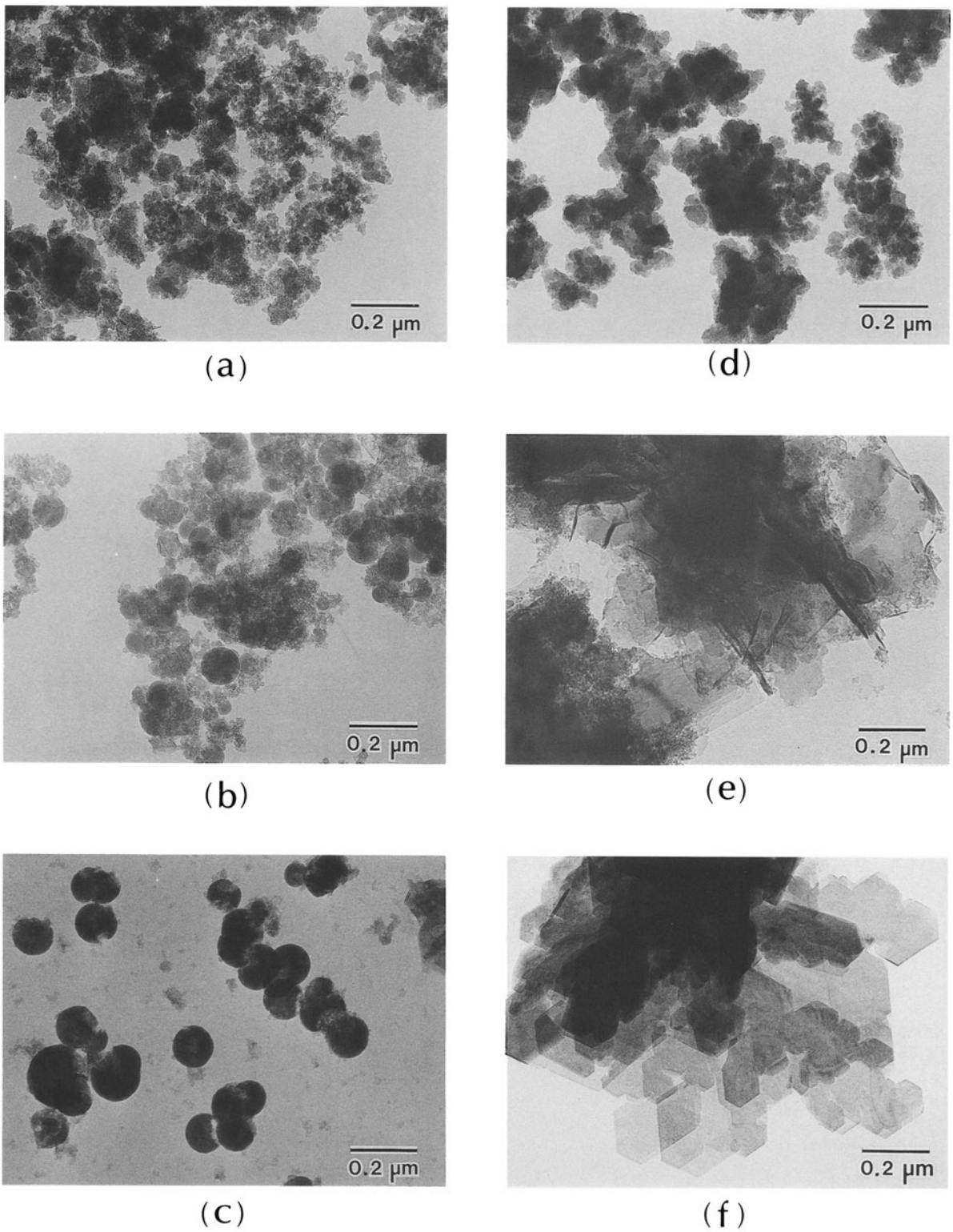

Figure 4. Transmission electron micrographs of a) gel-HA, the hydrothermal products for b) 1 day, and c) 9 days (product-A) from gel-HA, and d) gel-HB, the hydrothermal products for e) 5 days and for f) 9 days (product-B) from gel-HB.

https://doi.org/10.1346/CCMN.1994.0420307 Published online by Cambridge University Press

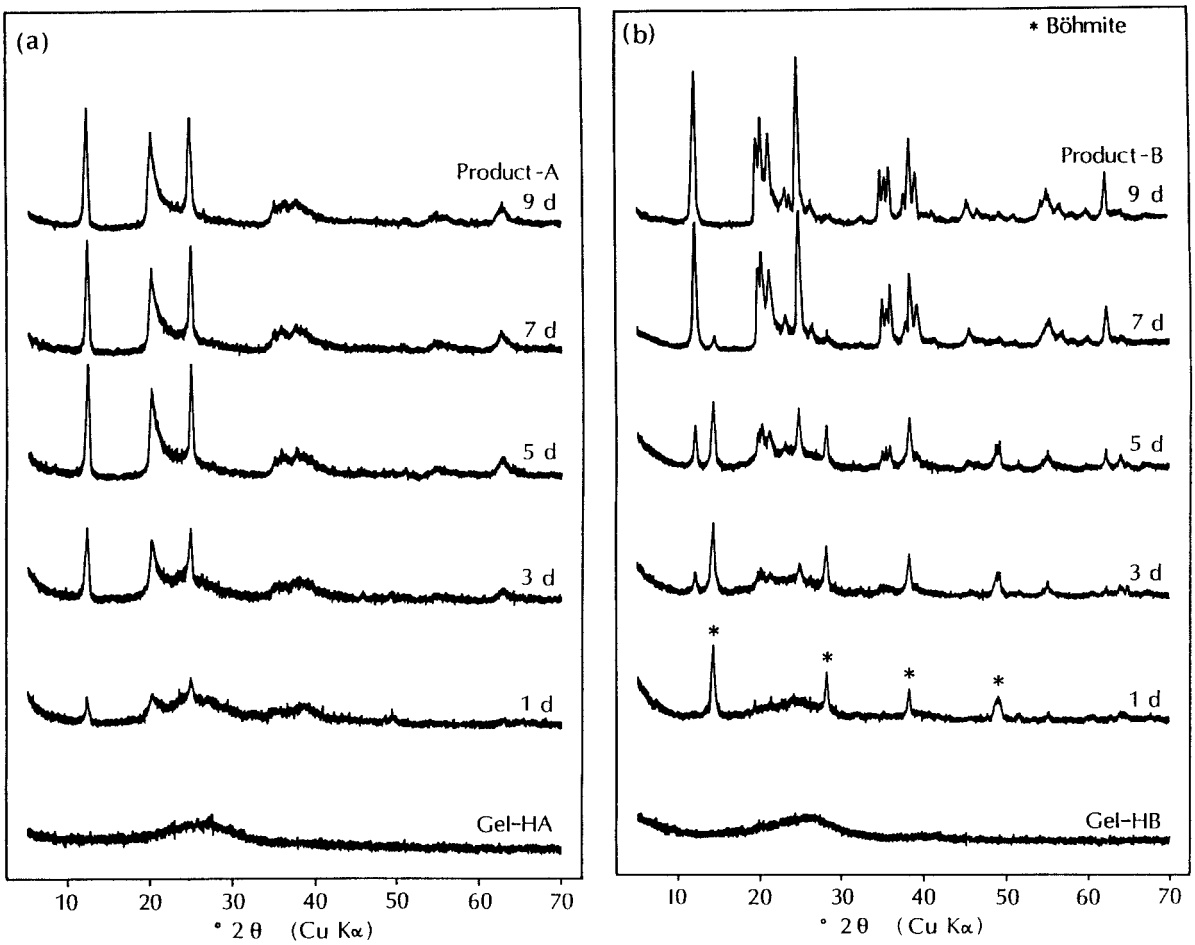

Figure 5. XRD patterns of the starting gels and the hydrothermal products: a) gel-HA and the products obtained from gel-HA; and b) gel-HB and the products obtained from gel-HB.

A"), as well as those obtained by the syntheses for 5 and 7 days, gave a broad asymmetrical non-basal diffraction band of kaolinite at approximately 4.5Å. The XRD patterns of gel-HB and its hydrothermal products are shown in Figure 5b. The peaks of boehmite were observed in the product obtained after 1 day. Weak peaks of kaolinite were apparent in the product obtained after 3-day reaction and their intensities increased with increasing reaction time. The product obtained by the hydrothermal reaction for 9 days (hereafter described as "product-B") gave only kaolinite diffraction peaks. Product-B showed non-basal diffractions at approximately 4.5Å sharper than those observed for product-A. The value of Hinckley's index for product-B was 0.98, whereas it could not be calculated for product-A because of its broad diffractions (Table 2). The d-value of 060/331 for product-A was slightly smaller than that of product-B, suggesting that the unit cell volume of product-A was slightly smaller than that of product-B (Table 2).

Table 2. Properties of products.

		Product A	Product B
TEM	Morphology	Sphere	Plate
XRD	Product	Kaolinite	Kaolinite
	d(001) (Å)	7.2	7.2
	d(060/331) (Å)	1.48	1.49
	Hinckley Index	n.d.[1]	0.98
TGA	Yield (%)	85	98
DTA	Endo. peak (°C)	530	550
	Exo. peak (°C)	990	994
BET	Surface area (m^2/g)	100	36

[1] Not detected.

Different morphologies were observed by TEM for products-A and-B (Figures 4c and 4f). A spherical shape was clearly observed for product-A, with diameters between 0.1 and 0.2 μm (Figure 4c). The shape was similar to that of the spherical kaolinite reported by Tomura *et al.* (1983). The spherical shape was also observed in the intermediate product reacted for 1 day (Figure 4b). On the other hand, platy crystals with a hexagonal shape were observed in product-B (Figure

https://doi.org/10.1346/CCMN.1994.0420307 Published online by Cambridge University Press

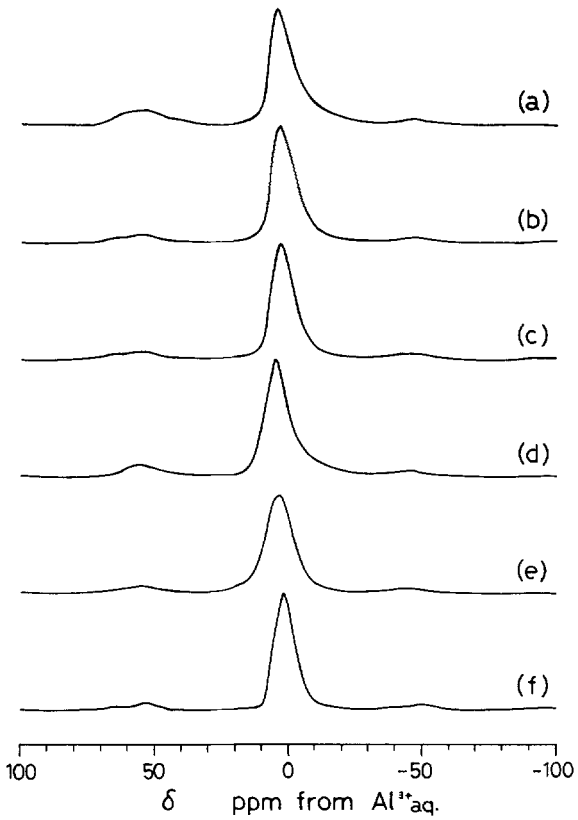

Figure 6. ^{27}Al-MAS/NMR spectra of the hydrothermal products for a) 1 day, b) 5 days, and c) 9 days (product-A) from gel-HA; and the products for d) 1 day, e) 5 days, and f) 9 days (product-B) from gel-HB.

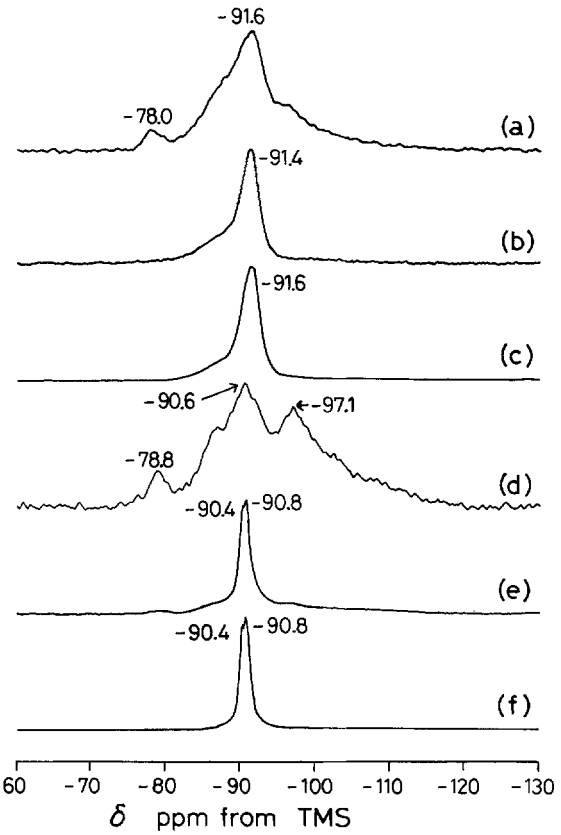

Figure 7. ^{29}Si-CP/MAS/NMR spectra of the hydrothermal products for a) 1 day, b) 5 days, and c) 9 days (product-A) from gel-HA, and the products for d) 1 day, e) 5 days, and f) 9 days (product-B) from gel-HB.

4f). The crystals with dimension less than 0.5 μm formed aggregates, and most of the aggregates were within the range of 1-2 μm in size (Figure 4f). No spherical particles could be observed in the products obtained by 5- and 9-day reaction of gel-HB (Figures 4e and 4f).

^{27}Al-MAS/NMR spectra of hydrothermal products (1, 5, and 9 days reaction of gels-HA and -HB) showed similar resonances at about 0–10 ppm corresponding to six-coordinated Al atoms (Figure 6). The slight difference of the profile of ^{27}Al resonances cannot be interpreted because the ^{27}Al signals are often complicated by quadrupolar effects.

^{29}Si-CP/MAS/NMR spectra of the products are shown in Figure 7. Each spectrum of the product obtained from gel-HA (Figures 7a-7c) showed a resonance at around -91 ppm as a main peak. The product of 1-day reaction (Figure 7a) had a small resonance at -78 ppm and a broad resonance ranging from -80 to -110 ppm in addition to the main resonance (-91.6 ppm). The resonance at -91.6 ppm of product-A corresponds to the characteristic chemical environment of Si atoms of spherical kaolinite, and its shoulder in low magnetic field side should be attributed to another amorphous phase in product-A. In contrast, the product obtained from gel-HB for 1-day reaction showed broad peaks ranging from -80 to -110 ppm with three maxima at -78.8, -90.6, and -97.1 ppm (Figure 7d). However, the products obtained by the syntheses for 5 and 9 days (product-B) gave sharp peaks at -90.4 and -90.8 ppm (Figures 7e and 7f). The doublet signal profile of product-B is identical to that of kaolinite with high crystallinity (Barron *et al.*, 1983).

Figure 8 shows the IR spectra of products-A and -B. Product-A had three peaks in the OH stretching region (3700–3600 cm^{-1}) (Van der Marel and Beutelspacher, 1976), and the absorption bands at 3696 and 3628 cm^{-1} were much stronger than that at 3656 cm^{-1}. On the other hand, product-B gave four peaks in the OH stretching region with clear resolution; the weaker absorption bands at 3670 and 3654 cm^{-1} were observed in addition to the stronger ones at 3694 and 3623 cm^{-1}. In the Si–O–Si (including Si–O–Al) antisymmetric stretching region (1200–950 cm^{-1}), product-A showed three peaks at 1120, 1054, and 1014 cm^{-1}, whereas product-B had four peaks at 1114, 1098,

https://doi.org/10.1346/CCMN.1994.0420307 Published online by Cambridge University Press

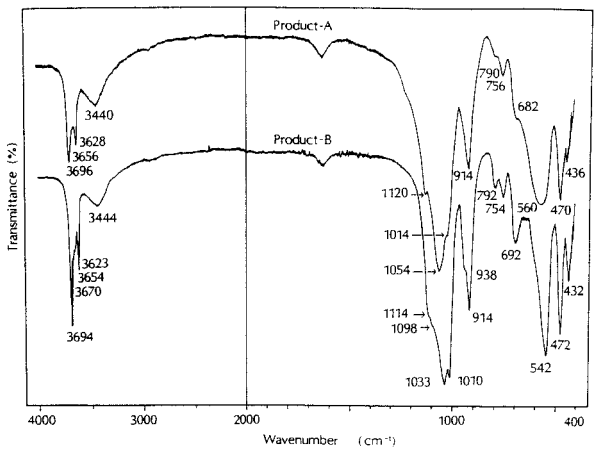

Figure 8. IR spectra of products-A and -B.

1033, and 1010 cm^{-1}. A singlet related to the Al–OH absorption band at 914 cm^{-1} was observed for product-A, in contrast to the doublet for product-B (938 and 914 cm^{-1}). Differences between products-A and B were also observed in the range of the Si–O–Si (including Si–O–Al) symmetric stretching absorption band (800–500 cm^{-1}). Product-A showed a weak absorption band at 682 cm^{-1} and a broad one at 560 cm^{-1}, in comparison to product-B showing two sharp bands at 692 and 542 cm^{-1}.

DTA curves of the gels and hydrothermal products are shown in Figures 9a and 9b. Both gels showed a broad endothermic peak below 300°C and a sharp exothermic peak between 990° and 1000°C. The intensities of the exothermic peaks of both gels decreased within 1-day reaction, but they increased with increasing duration of the reaction for more than 1 day. Kaolinite has an endothermic peak in the 500°–700°C region due to the dehydration of structural OH groups and an exothermic peaks lies between 950° and 980°C corresponded to the formation of mullite on the DTA curve (Holdridge and Vaughan, 1957). The endothermic and exothermic peaks of product-A were observed at lower temperatures than those of product-B (Table 2). Moreover, the profile of the endothermic peak of product-A showed asymmetrical broadening on the lower temperature side. The yield of kaolinite in the product was estimated from the weight loss recorded on the TG curve between 400° and 1100°C which corresponds to the dehydration of structural OH groups of kaolinite. The yield of kaolinite in product-A was 85% and that in product-B was 98%. The remainder of each product should be present as an amorphous phase.

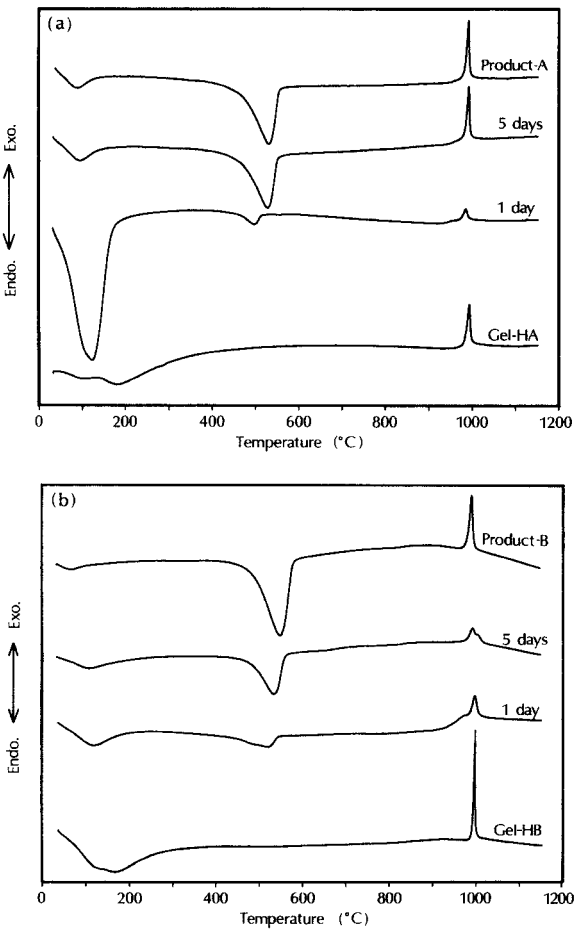

Figure 9. DTA curves of a) gel-HA and its hydrothermal products and b) gel-HB and its hydrothermal products.

Table 3. The pH values, surface area, and atomic ratios of gels and hydrothermal products.

Reaction time (days)	pH		Surface area (m^2/g)		Si/Al	
	Gel-HA	Gel-HB	Gel-HA	Gel-HB	Gel-HA	Gel-HB
—	6.4	5.2	40	246	1.06	1.18
1	5.4	3.4	474	466	1.05	1.00
3	4.9	2.7	307	367	1.05	1.01
5	4.9	3.0	186	308	1.07	1.03
7	4.9	1.6	160	53	1.08	1.02
9	5.0	1.7	100	36	1.09	1.02

Table 3 gives the pH values of the slurries before and after the hydrothermal reactions. The pH values of both reactions showed a tendency to decrease within 1 day and, subsequently, to decrease gradually with increasing duration of the reaction.

The specific surface areas of the gels and their hydrothermal products are given in Table 3. The specific surface areas of the products obtained from both gels by the reaction for 1 day were larger than those of gels-HA and -HB, and the specific surface areas decreased within the course of crystallization. A remarkable decrease in the specific surface area was observed between 5 and 7 days in the reaction of gel-HB, whereas the specific surface areas of the products obtained from

https://doi.org/10.1346/CCMN.1994.0420307 Published online by Cambridge University Press

gel-HA were gradually reduced throughout the crystallization process.

The atomic ratios of Si/Al calculated from the analytical data of the chemical compositions are also given in Table 3. The Si/Al ratio for product-A was 1.09 and that for product-B was 1.02. The Si/Al ratios of the products were closer to the theoretical ratio of kaolinite than those of both ion-exchanged gels.

Hydrothermal reaction under originally low pH

The XRD pattern of the product from gel-HA under initially acid condition was given in Figure 10. The final pH value was 2.2, and slight amounts of pseudoböhmite and kaolinite were formed after the reaction for 9 days.

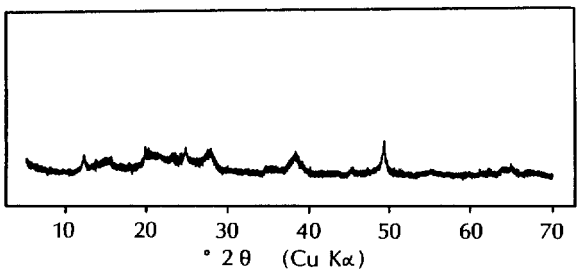

Figure 10. XRD pattern of the product from gel-HA obtained under the low pH condition.

DISCUSSION

The structure of starting gels

The ^{27}Al-MAS/NMR spectra showed the difference in the coordination numbers of Al atoms between gels-A and -B (Figures 2a and 2c). After the removal of the impurities, a part of four-coordinated Al atoms in gel-A changed to six-coordinated ones (gel-HA) (Figure 2b). The change in coordination of Al atoms in gel-A could be caused by the hydration of the gel due to the exchange of Na ions for hydronium ions (Léonard *et al.*, 1964). This interpretation is supported by the TG data showing that the water content in gel-HA was larger than that in gel-A. The chemical shift of the ^{29}Si-MAS/NMR peak is affected by the polycondensation state of SiO_4 tetrahedra and the number of AlO_4 tetrahedra linked to an SiO_4 tetrahedron (Lippmaa *et al.*, 1981). Therefore, the chemical shift of gel-A (−82 ppm) (Figure 3a) is attributed to Q^2, Q^3(2Al), or Q^4(4Al) states (Watanabe and Shimizu, 1986; Lippmaa *et al.*, 1981; Thompson *et al.*, 1992). The four-coordinated Al atoms in gel-A, which were detected by the ^{27}Al-MAS/NMR, and the chemical composition of gel-A (Table 1) suggest the structure of gel-A probably consists of networks of the alternation of SiO_4- and AlO_4-tetrahedra with the Q^4(4Al) state as a main component. The ^{29}Si-CP/MAS/NMR resonance of gel-HA from −75 to −110 ppm centered at −93 ppm is so broad that it is probably an overlap of Q^3, Q^4(2Al), Q^4(3Al), Q^4(4Al), and maybe even others (Figure 3b). After the ion-exchange treatment, some of the hydrated Al atoms in gel-HA might be released from the networks in gel-A and the gel structure should be appreciably modified.

The ^{27}Al-MAS/NMR and ^{29}Si-CP/MAS/NMR spectra of gels-B and -HB are similar to each other, respectively (Figures 2c and 2d, and 3c and 3d). The structure of gel-B is not appreciably modified by the ion-exchange treatment. Therefore, Na ions in gel-B should be out of the framework of gel-B and they were removed easily. The ^{29}Si-CP/MAS/NMR spectra of gel-B consists of two peaks, one is a narrow resonance at −78 ppm and the other is a broad peak from −75 to −110 ppm (Figure 3c). The narrow resonance was ascribed to Si tetrahedra which are attached to one hydrogen and three Al octahedra through oxygen, i.e., $Si(OAl_{oct})_3OH$ (Barron *et al.*, 1982). The broad peak should consist of some resonances that are ascribed to some Si sites, Q^3, Q^4(2Al), Q^4(3Al), and Q^4(4Al) (Lippmaa *et al.*, 1980). The ^{29}Si resonance of gels-B and -HB are similar to previously reported spectra of synthetic allophane (Wilson *et al.*, 1988) and poorly ordered aluminosilicates containing proto-imogolite (Wilson *et al.*, 1986). Therefore, the local structure of gels-B and -HB would be closely related to the structures of allophanes and/or the poorly ordered aluminosilicates containing proto-imogolite. Recently, MacKenzie *et al.*, (1991) presented the structural model of allophanes. A "two-sheet," kaolinite-like structure containing defects, is curved into a sphere in which imogolite-like orthosilicate units are anchored into the octahedral sheet and fit into the tetrahedral defects. Gels-B and -HB, therefore, may have the similar sheet structure to those of allophanes.

Properties of kaolinite

The XRD pattern of product-A shows the sharp basal diffractions and the broad non-basal diffractions (Figure 5a). Such a pattern can be observed for 7 Å halloysite and the spherical kaolinite (Tomura *et al.*, 1983). They suggested that spherical halloysite changes its original morphology with smoothly curved surface to polyhedral morphology consisting of depressed facets due to dehydration under a vacuum condition for the TEM observation, whereas spherical kaolinite does not show such a morphological change. The transmission electron micrographs of product-A clearly showed spherical particles with smooth surface (Figure 4c). Moreover, it is impossible for halloysite to form at such high reaction temperatures (Roy and Osborn, 1954). Consequently, the spherical particles in product-A are spherical kaolinite, but not halloysite.

The XRD pattern of product-B (Figure 5b) was a typical pattern of well-ordered kaolinite and its Hinckley's index was 0.98. The hexagonal plate in the TEM (Figure 4f) is a typical morphology of platy kaolinite.

https://doi.org/10.1346/CCMN.1994.0420307 Published online by Cambridge University Press

Hydrothermal reaction process

Two kinds of products with different morphologies were obtained in the present study. There are two possible reasons for the difference; one is the pH values of the reaction systems and the other is the effect of the structures of the starting gels. The degree of acidification was more severe in the system with the gel-HB (Table 3). The decrease in the pH values is mainly caused by the sulfate ions originating from the initial gel. De Kimpe *et al.* (1964) and Miyawaki *et al.* (1989) reported that the synthesis of kaolinite was affected by the pH condition of the reaction system. Therefore, the hydrothermal reaction of gel-HA was examined under low pH, which was adjusted to the final pH value of the product-B (about pH = 2) with additional sulfuric acid. However, kaolinite was hardly formed even after 9 days reaction under the low pH condition. This result suggests that the morphology is not simply affected by pH value alone.

The product of the hydrothermal reaction of gel-HA for 1 day gave a larger specific surface area than that of the starting material, gel-HA (Table 3). The thermal analysis showed that the water content in this product was much higher than that in gel-HA (Figure 9a). This product gave weak XRD peaks of kaolinite (Figure 5a), and a weak resonance at −78 ppm ascribed to the silicon tetrahedra with one hydroxide in ^{29}Si-CP/MAS/NMR spectrum (Figure 7a). Therefore, this product should consist of a highly hydrated amorphous aluminosilicate, an intermediate phase of kaolinitization derived from gel-HA. The exothermic peak at approximately 990°C of this product, which is weaker than those of gel-HA and product-A, should substantiate the existence of the intermediate phase. The transition from the intermediate amorphous to kaolinite started as early as 1-day reaction. Tomura *et al.* (1985) showed that spherical kaolinite was produced in a highly supersaturated solution of silica and alumina. It can, therefore, be presumed that the spherical kaolinite in this study should be precipitated owing to the supersaturation of a silica-alumina cluster derived from the intermediate phase.

On the other hand, the product obtained from gel-HB within 1-day reaction gave a larger specific surface area than that of gel-HB, but the XRD pattern of this product showed the presence of boehmite as an intermediate phase. Tsuzuki (1976) described that the sequence of precipitation of phases, boehmite → kaolinite → amorphous silica plus kaolinite, from a solution of silica and alumina could be shown in the solubility diagrams defined by log [Al^{3+}] and log [H_4SiO_4] at 200°C and pH = 4. ^{29}Si-CP/MAS/NMR spectrum of the product of 1-day reaction showed the existence of several kinds of Si chemical environments. The chemical shifts of −78.8 ppm, −90.6 ppm, and −97.1 ppm should be ascribed to $Si(OAl_{oct})_3OH$ in the imogolite-like structure, $Q^3(1Al_{oct})$ in a kaolinite-like structure, and Q^3 species of an amorphous silica derived from gel-HB, respectively (Lippmaa *et al.*, 1981). It is speculated that Al atoms released from a part of gel-HB to form boehmite, then the crystallization of kaolinite should be promoted by the reaction of boehmite with the dissolved silica. Kaolinite with platy morphology in product-B should be crystallized on the basis of the sheet structure of the boehmite.

CONCLUSION

By the hydrothermal reaction at 220°C for 9 days, spherical kaolinite was synthesized from the gel prepared at pH 9.6 having an alternation of SiO_4- and AlO_4-tetrahedra, and platy kaolinite was synthesized from the gel prepared at pH 4.2 having allophane-like and/or proto-imogolite structures. There were two kinds of intermediate phases depending on the starting gel before the crystallization of kaolinite. The crystallization of spherical kaolinite was started in 1 day and then gradually crystallized through the amorphous aluminosilicate with great water content, whereas the platy kaolinite was crystallized after the precipitation of boehmite.

ACKNOWLEDGMENTS

The authors are grateful to Prof. Kazuyuki Kuroda of Waseda University for his kind suggestions. We thank Dr. Yuji Tokunaga and Mrs. Fumie Shimada of the chemical research laboratory, Tosoh Corporation, for their technical assistance with the TEM analysis. We express appreciation to Mr. Yukihiro Tsutsumi, the manager of the chemical research laboratory, Tosoh Corporation, for his encouragement. A part of this study was supported by the special research program for important regional technology, Agency of Industrial Science and Technology, Ministry of International Trade and Industry, Japan.

REFERENCES

Barron, P. F., Wilson, M. A., Campbell, A. S., and Frost, R. L. (1982) Detection of imogolite in soils using solid state ^{29}Si NMR: *Nature* **299,** 616–618.

Barron, P. F., Frost, R. L., Skjemstad, J. O., and Koppi, A. J. (1983) Detection of two silicon environments in kaolins by solid-state ^{29}Si NMR: *Nature* **302,** 49–50.

Cloos, P., Léonard, A. J., Moreau, J. P., Herbillon, A., and Fripiat, J. J. (1969) Structural organization in amorphous silico-aluminas: *Clays & Clay Minerals* **17,** 279–287.

De Kimpe, C., Gastuche, M. C., and Brindley, G. W. (1961) Ionic coordination in alumino-silicic gels in relation to clay mineral formation: *Amer. Mineral.* **46,** 1370–1381.

De Kimpe, C. and Gastuche, M. C. (1964) Low-temperature syntheses of kaolin minerals: *Amer. Mineral.* **49,** 1–16.

Ewell, R. H. and Insley, H. (1935) Hydrothermal synthesis of kaolinite, dickite, beidellite, and nontronite: *J. Res. Nat. Bur. Stand.* **15,** 173–186.

Fripiat, J. J., Léonard, A., and Uytterhoeven, J. B. (1965) Structure and properties of amorphous silicoaluminas. II. Lewis and brønsted acid sites: *J. Phys. Chem.* **69,** 3274–3279.

Holdridge, D. A. and Vaughan, F. (1957) The kaolin minerals (Kandites): in *The Differential Thermal Investigation of Clays,* R. C. Mackenzie, ed., Mineralogical Society, London, 98–139.

Léonard, A., Suzuki, Sho., Fripiat, J. J., and De Kimpe, C. (1964) Structure and properties of amorphous silicoaluminas. I. Structure from X-ray fluorescence spectroscopy and infrared spectroscopy: *J. Phys. Chem.* **68,** 2608–2617.

Lippmaa, E., Mägi, M., Samoson, A., Engelhardt, G., and Grimmer, A.-R. (1980) Structural studies of silicates by solid-state high-resolution ^{29}Si NMR: *J. Am. Chem. Soc.* **102,** 4889–4893.

Lippmaa, E., Mägi, M., Samoson, A., Tarmak, M., and Engelhardt, G. (1981) Investigation of the structure of zeolites by solid-state high-resolution ^{29}Si NMR spectroscopy: *J. Am. Chem. Soc.* **103,** 4992–4996.

MacKenzie, K. J. D., Bowden, M. E., and Meinhold, R. H. (1991) The structure and thermal transformations of allophanes studied by ^{29}Si and ^{27}Al high resolution solid-state NMR: *Clays & Clay Minerals* **39,** 337–346.

Miyawaki, R., Tomura, S., Shibasaki, Y., and Samejima, S. (1989) Appropriate pH for hydrothermal synthesis of kaolinite from amorphous mixture of alumina and silica: *Reports of the Government Industrial Research Institute, Nagoya* **38,** 330–335 (in Japanese with English abstract).

Miyawaki, R., Tomura, S., Samejima, S., Okazaki, M., Mizuta, H., Maruyama, S., and Shibasaki, Y. (1991) Effects of solution chemistry on the hydrothermal synthesis of kaolinite: *Clays & Clay Minerals,* **39,** 498–508.

Pourbaix, M., ed. (1991) *Atlas of Electrochemicals in Aqueous Solutions:* Pergamon Press, New York, 168–176, 458–463 pp.

Roy, R. and Osborn, E. F. (1954) The system Al_2O_3-SiO_2-H_2O: *Amer. Mineral.* **39,** 853–885.

Thompson, J. G., Philippa, J. R. U., Whittaker, A. K., and Mackinnon, I. D. R. (1992) Structural characterization of kaolinite:NaCl intercalate and its derivatives: *Clays & Clay Minerals,* **40,** 369–380.

Tomura, S., Shibasaki, Y., Mizuta, H., and Kitamura, M. (1983) Spherical kaolinite: Synthesis and mineralogical properties: *Clays & Clay Minerals* **31,** 413–421.

Tomura, S., Shibasaki, Y., Mizuta, H., and Kitamura, M. (1985) Growth conditions and genesis of spherical and platy kaolinite: *Clays & Clay Minerals* **33,** 200–206.

Tsuzuki, Y. (1976) Solubility diagrams for explaining zone sequences in bauxite, kaolin and pyrophyllite-diaspore deposits: *Clays & Clay Minerals* **24,** 297–302.

Van der Marel, H. W. and Beutelspacher, H., eds. (1976) *Atlas of Infrared Spectroscopy of Clay Minerals and Their Admixtures:* Elsevier, New York, 65–93.

Watanabe, T. and Shimizu, H. (1986) High resolution solid state NMR and its application to clay minerals: *J. Mineral Soc. Jpn.* **17,** 123–136 (special issue, in Japanese with English abstract).

Wilson, M. A., McCarthy, S. A., and Fredericks, P. M. (1986) Structure of poorly-ordered aluminosilicates: *Clay Miner.* **21,** 879–897.

Wilson, M. A., Wada, K., Wada, S. I., and Kakuto, Y. (1988) Thermal transformations of synthetic allophane and imogolite as revealed by nuclear magnetic resonance: *Clay Miner.* **23,** 175–190.

(Received 18 January 1993; accepted 22 December 1993; Ms. 2310)